

# Reaction Mechanism of CO<sub>2</sub> Methanation

Subjects: [Chemistry](#), [Physical](#)

Contributor: Li Li

The combustion of fossil fuels has led to a large amount of carbon dioxide emissions and increased greenhouse effect. Methanation of carbon dioxide can not only mitigate the greenhouse effect, but also utilize the hydrogen generated by renewable electricity such as wind, solar, tidal energy, and others, which could ameliorate the energy crisis to some extent. Highly efficient catalysts and processes are important to make CO<sub>2</sub> methanation practical. Although noble metal catalysts exhibit higher catalytic activity and CH<sub>4</sub> selectivity at low temperature, their large-scale industrial applications are limited by the high costs. Ni-based catalysts have attracted extensive attention due to their high activity, low cost, and abundance. At the same time, it is of great importance to study the mechanism of CO<sub>2</sub> methanation on Ni-based catalysts in designing high-activity and stability catalysts.

[CO<sub>2</sub>](#)[CH<sub>4</sub>](#)[reaction mechanism](#)[Ni-based catalysts](#)[low temperature](#)

## 1. Introduction

With the continuous advancement of social economy and the unceasing enhancement of human living standards, the overuse of fossil fuels has resulted in an energy crisis while the excessive emission of CO<sub>2</sub> has exacerbated the greenhouse effect, which has induced global climate problems [\[1\]\[2\]\[3\]\[4\]\[5\]](#). As the main component of industrial waste gas, CO<sub>2</sub> could also be used as an abundant and cheap chemical feedstock for renewable fuels [\[6\]](#). Therefore, converting CO<sub>2</sub> into value-added chemicals is considered to be one of the most promising strategies to mitigate the energy crisis and reduce the greenhouse effect. Several clean and renewable energy resources such as wind, solar, and tidal energy produce discontinuous and unstable electricity, which cannot be used effectively. Hydrogen can be generated by the electrolysis of water using this kind of unstable electricity [\[7\]\[8\]\[9\]\[10\]\[11\]](#). With this low cost H<sub>2</sub> supply, CO<sub>2</sub> could be hydrogenated to form methane [\[12\]\[13\]\[14\]\[15\]](#), and methane, as the main component of natural gas, can be effectively utilized as a fuel or chemical, thus forming a new carbon cycle. In light of the importance of the CO<sub>2</sub> methanation reaction, it has been widely investigated. This reaction was proposed by Sabatier and Senderens in 1902, which was also called the Sabatier reaction (Equation (1)) [\[16\]\[17\]](#). The reaction is exothermic, and can be carried out at low temperature to achieve high CO<sub>2</sub> conversion [\[18\]\[19\]\[20\]\[21\]](#). However, CO<sub>2</sub> is the upmost oxidized state of carbon and the activation of the C–O bond in CO<sub>2</sub> faces many challenges. The hydrogenation of CO<sub>2</sub> to methane is an eight-electron process with high kinetic barrier that requires a catalyst to achieve acceptable rates and selectivity [\[22\]\[23\]\[24\]](#). The active metals usually affect the catalytic activity and selectivity of the catalysts. Many noble metals such as Rh [\[2\]\[25\]](#), Ru [\[26\]\[27\]\[28\]](#), and Pd [\[29\]\[30\]](#) have been widely applied in CO<sub>2</sub> methanation due to their excellent activity and CH<sub>4</sub> selectivity at low temperature. However, their large-scale industrial

applications are limited due to the high costs. In addition to noble metal catalysts, some Ni-based catalysts also exhibit high catalytic activity and CH<sub>4</sub> selectivity. However, the precise elucidation of the CO<sub>2</sub> methanation mechanism is still a challenging task. It is crucially important to understand the key intermediates and reaction mechanisms in depth when designing catalysts with excellent catalytic performance [26].



## 2. The Reaction Mechanism of CO<sub>2</sub> Methanation

Many researchers have made efforts to elucidate the possible CO<sub>2</sub> methanation mechanism by in situ FTIR, mass spectrometry (transient-MS) techniques, and DFT calculations. Although there are many arguments on the intermediates and different reaction pathways of CH<sub>4</sub> formation, two widely accepted pathways have been proposed: (1) the formate pathway where formate species are the main intermediate products formed during CO<sub>2</sub> methanation reaction, also called the CO<sub>2</sub> associative methanation: the chemisorbed \*CO<sub>2</sub> species can first be converted to bidentate formates (HCOO\*) and then to formic acid (HCOOH), then to CH<sub>4</sub>, and (2) the CO pathway, also called the CO<sub>2</sub> dissociative methanation: the chemisorbed \*CO<sub>2</sub> species can dissociate into \*CO and \*O. The formed \*CO species can further dissociate into carbon species (\*C), which can then be hydrogenated to CH<sub>4</sub> by dissociated H<sub>2</sub> still on the metal particles, desorbing from the catalyst surface, whereas the \*O species can react with hydrogen to produce H<sub>2</sub>O [10][31][32][33][34][35][36].

The possible reaction pathways are illustrated in **Figure 1**. CO<sub>2</sub> methanation on different catalysts occur via two different pathways, which are affected by the nature of nickel active sites and the supports [10].

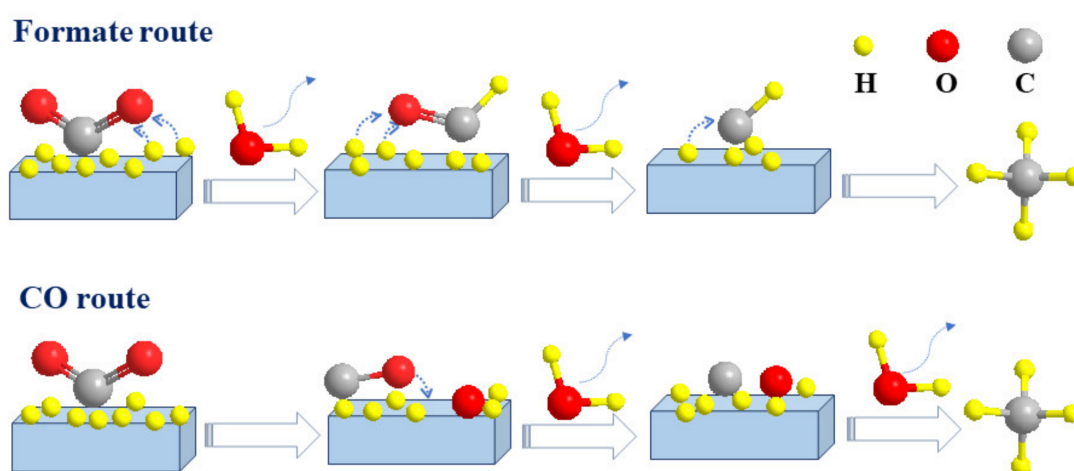


**Figure 1.** Two different CO<sub>2</sub> methanation reaction routes: formate route and CO route.

### 2.1. The Formate Pathway

Many studies have reported that CO<sub>2</sub> methanation follows the formate route on different nickel catalysts such as Ni/MgO [37], Ni-Mn/Al@Al<sub>2</sub>O<sub>3</sub> [38], Ni/Y<sub>2</sub>O<sub>3</sub> [39], Ni/ZrO<sub>2</sub> [35][40], Ni/ultra-stable Y (USY) zeolite [41], and Ni@C [42]. For

example, Xu and coworkers [35] discussed the formation and evolution of CO<sub>2</sub> adsorbed species on Ni/c-ZrO<sub>2</sub> by in situ FTIR and DFT calculations. CO<sub>2</sub> methanation on Ni/c-ZrO<sub>2</sub> was dominated by the formate pathway as follows: CO<sub>2</sub>\* → HCOO\* → H<sub>2</sub>COO\* → H<sub>2</sub>COOH\* → H<sub>2</sub>CO\* → CH<sub>2</sub>\* → CH<sub>4</sub>\*, which is the same as that shown in **Figure 1**. CO was a by-product instead of a reaction intermediate, which could not further form CH<sub>4</sub>, and the DFT calculations also confirmed the formate pathway, which was highly consistent with the in situ FTIR results. Solis-Garcia et al. [40] also found that CO<sub>2</sub> methanation follows the formate pathway over Ni/ZrO<sub>2</sub> and no CO species were observed during the reaction. The possible reaction pathway of the CO<sub>2</sub> methanation over Ni@C was also investigated by CO<sub>2</sub>-TPD measurements and in situ FTIR characterization. All results demonstrated that CO<sub>2</sub> methanation over Ni@C catalyst proceeded via the formate route without involving CO as an intermediate [42]. Aldana et al. [12] also found that the main CO<sub>2</sub> methanation mechanism on Ni-CZ<sub>sol-gel</sub> was the formate pathway, which does not require CO as reaction intermediate. They also found that H<sub>2</sub> was dissociated on Ni<sup>0</sup> sites while CO<sub>2</sub> was activated on the ceria–zirconia support to form carbonates and then further into CH<sub>4</sub>, suggesting that a stable metal–support interface is beneficial for the adsorption of CO<sub>2</sub>.

In another study, Pan et al. [43] found that the reaction pathway on Ni/γ-Al<sub>2</sub>O<sub>3</sub> and Ni/Ce<sub>0.5</sub>Zr<sub>0.5</sub>O<sub>2</sub> all followed the formate pathway, only differing in reactive basic sites. On the Ni/Ce<sub>0.5</sub>Zr<sub>0.5</sub>O<sub>2</sub> catalyst, CO<sub>2</sub> adsorption on medium basic sites formed bidentate formate, whereas CO<sub>2</sub> adsorption on surface oxygen resulted in the monodentate formate. Due to the faster hydrogenation of monodentate formate, it was assumed to be the main reaction route on the Ni/Ce<sub>0.5</sub>Zr<sub>0.5</sub>O<sub>2</sub> catalyst. For CO<sub>2</sub> methanation on Ni/γ-Al<sub>2</sub>O<sub>3</sub>, hydrogenation of bidentate formate was the main reaction route as bidentate formate was the main adsorption and intermediate species and CO<sub>2</sub> adsorbed on strong basic sites of Ni/γ-Al<sub>2</sub>O<sub>3</sub> will not participate in the CO<sub>2</sub> methanation reaction. It was assumed that medium basic sites are responsible for promoting the formation of monodentate formate species, thus enhancing CO<sub>2</sub> methanation activity. CO<sub>2</sub> methanation reaction pathways on Ni/Ce<sub>0.5</sub>Zr<sub>0.5</sub>O<sub>2</sub> and Ni/γ-Al<sub>2</sub>O<sub>3</sub> are shown in **Figure 2**.

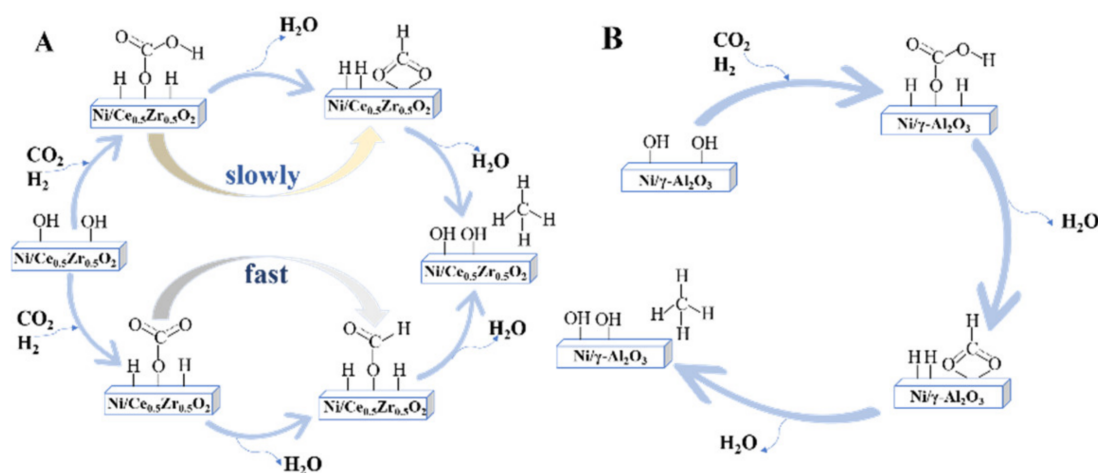


**Figure 2.** CO<sub>2</sub> methanation reaction route on (A) Ni/Ce<sub>0.5</sub>Zr<sub>0.5</sub>O<sub>2</sub> and (B) Ni/γ-Al<sub>2</sub>O<sub>3</sub>.

## 2.2. The CO Pathway

The CO pathway involves the dissociation of CO<sub>2</sub> to CO prior to methanation, and in the subsequent reaction, CO is converted to CH<sub>4</sub> by reacting with H<sub>2</sub> [44]. Karelavic et al. showed the direct dissociation of CO<sub>2</sub>. The reactions below summarize the reduction process (Equations (3) and (4)). The excess amount of CO generated in the first reaction deposits on the catalyst, which produces coking effects. To avoid this problem, the methanation of CO must proceed much faster than the CO production, and the CO<sub>2</sub> methanation reaction must take place at low temperatures. Therefore, the direct dissociation of CO<sub>2</sub> to CO<sub>ads</sub> and O<sub>ads</sub> often occur over a variety of noble metal-based catalysts at low temperature [25][45][46]. In addition, the formation of nickel carbonyls Ni(CO)<sub>4</sub> would cause the deactivation of Ni-based catalysts [47].



Therefore, CO<sub>2</sub> methanation occurred via the CO pathway only over some Ni-based catalysts including Ni/CeO<sub>2</sub> [48], Ni/F-SBA-15 [49], and Ni-sepiolite [50]. The CO pathway over Ni/CeO<sub>2</sub> could be proven by in situ FTIR. The FTIR adsorption bands at 2017 cm<sup>-1</sup> were assigned to the CO adsorption state, and the bands at 2120 and 2170 cm<sup>-1</sup> were ascribed to gas phase CO, which indicated that CO<sub>2</sub> molecules can be converted to CO molecules on the surface of the Ni/CeO<sub>2</sub> catalyst. Characterization results indicated that CO species generated from the reduction of CO<sub>2</sub> molecules by nickel active sites and surface oxygen vacancies promoted CO<sub>2</sub> methanation [48]. Bukhari et al. found that Ni metals on Ni/F-SBA-15 (Fibrous type SBA-15) contributed to the CO<sub>2</sub> dissociation into CO and O species as well as the dissociation of H<sub>2</sub> into atomic hydrogen species. The linear carbonyl group came from the dissociation of CO<sub>2</sub>, which was an intermediate during CO<sub>2</sub> methanation and could be seen at 2055 cm<sup>-1</sup>. Then, the adsorbed CO species interacted with surface oxygen, producing bidentate and unidentate carbonate groups, thus CH<sub>4</sub> [49]. Cerdá-Moreno et al. [50] also found linearly and bridged bonded CO as intermediates during CO<sub>2</sub> methanation over a Ni-sepiolite catalyst.

### 2.3. The Key Factors of CO<sub>2</sub> Methanation Reaction Route

There are also many factors influencing the CO<sub>2</sub> methanation mechanism. The addition of promoters affects the formation of intermediates. Mg or Ca modified Ni/Al<sub>2</sub>O<sub>3</sub> catalysts promote the formation of the carbonate species due to the increased basicity, while Sr or Ba modified catalysts promoted \*CO and H<sub>2</sub>CO\* formation [51]. The nature of nickel active sites also influence the CO<sub>2</sub> methanation mechanism. Zhou et al. [52] found that CO<sub>2</sub> methanation took the pathway of CO over the Ni/TiO<sub>2</sub> catalyst with Ni (111) as the principal exposing facet, while the catalyst with multi-facets followed the formate route, with which nickel was only functional for hydrogen dissociation. The location of nickel active sites also affects the CO<sub>2</sub> methanation reaction pathways [33]. Controlling nickel being on either the interior or the exterior of adjacent siloxene nanosheets is achieved by employing different solvents in the preparation process, which determines the reaction intermediates and pathways for CO<sub>2</sub> methanation, as shown in **Figure 3**. CO<sub>2</sub> methanation occurred through the formate pathway over Ni@SiXNS-EtOH with nickel active sites being on the interior of adjacent siloxene nanosheets while CO<sub>2</sub> methanation followed the CO pathway when nickel was at the exterior of adjacent siloxene nanosheets on Ni@SiXNS-H<sub>2</sub>O.

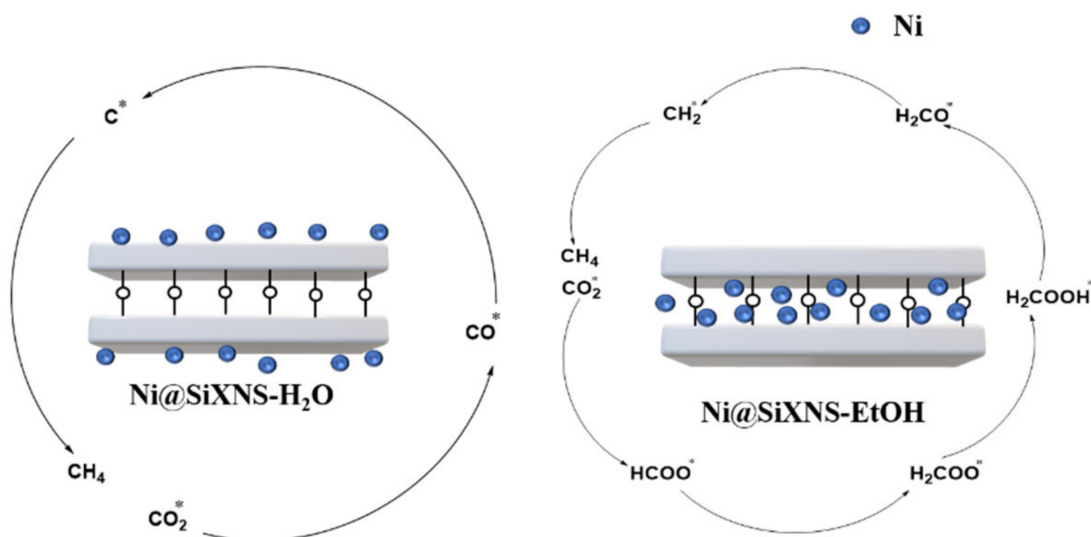


**Figure 3.** CO<sub>2</sub> methanation pathways on (A) Ni@SiXNS-H<sub>2</sub>O and (B) Ni@SiXNS-EtOH.

The different preparation methods can also influence the reaction pathway of CO<sub>2</sub> methanation. Jia et al. [53] used the *operando* DRIFT analyses to demonstrate the CO<sub>2</sub> methanation pathway on Ni/ZrO<sub>2</sub> obtained via different preparation methods. CO<sub>2</sub> methanation over the plasma decomposed catalyst follows the Co-hydrogenation route. The exposed high-coordinate Ni (111) facets of the plasma decomposed catalyst facilitate the decomposition of CO<sub>2</sub> and formates into adsorbed CO. The subsequent hydrogenation of adsorbed CO leads to the production of methane. However, the thermally decomposed catalyst with a complex Ni crystal structure and more defects mainly takes the pathway of direct formate hydrogenation.

## References

1. Anwar, M.N.; Fayyaz, A.; Sohail, N.F.; Khokhar, M.F.; Baqar, M.; Yasar, A.; Rasool, K.; Nazir, A.; Raja, M.U.F.; Rehan, M.; et al. CO<sub>2</sub> utilization: Turning greenhouse gas into fuels and valuable products. *J. Environ. Manag.* 2020, 260, 110059.
2. Yang, Y.; Liu, J.; Liu, F.; Wu, D. Reaction mechanism of CO<sub>2</sub> methanation over Rh/TiO<sub>2</sub> catalyst. *Fuel* 2020, 276, 118093.
3. Burger, T.; Koschany, F.; Thomys, O.; Köhler, K.; Hinrichsen, O. CO<sub>2</sub> methanation over Fe- and Mn-promoted co-precipitated Ni-Al catalysts: Synthesis, characterization and catalysis study. *Appl. Catal. A Gen.* 2018, 558, 44–54.
4. Ahadzi, E.; Ramyashree, M.; Priya, S.S.; Sudhakar, K.; Tahir, M. CO<sub>2</sub> to green fuel: Photocatalytic process optimization study. *Sustain. Chem. Pharm.* 2021, 24, 100533.
5. Silva, T.C.D.; Isha, A.; Chandra, R.; Vijay, V.K.; Subbarao, P.M.V.; Kumar, R.; Chaudhary, V.P.; Singh, H.; Khan, A.A.; Tyagi, V.K.; et al. Enhancing methane production in anaerobic digestion

- through hydrogen assisted pathways—A state-of-the-art review. *Renew. Sustain. Energy Rev.* 2021, 151, 111536.
6. Hussain, M.; Akhter, P.; Russo, N.; Saracco, G. Novel Ti-KIT-6 material for the photocatalytic reduction of carbon dioxide to methane. *Catal. Commun.* 2013, 36, 58–62.
  7. Li, S.; Guo, S.; Gong, D.; Kang, N.; Fang, K.-G.; Liu, Y. Nano composite composed of MoO<sub>x</sub>-La<sub>2</sub>O<sub>3</sub>-Ni on SiO<sub>2</sub> for storing hydrogen into CH<sub>4</sub> via CO<sub>2</sub> methanation. *Int. J. Hydrogen Energy* 2019, 44, 1597–1609.
  8. Alarcón, A.; Guilera, J.; Díaz-López, J.A.; Andreu, T. Optimization of nickel and ceria catalyst content for synthetic natural gas production through CO<sub>2</sub> methanation. *Fuel Process. Technol.* 2019, 193, 114–122.
  9. Xing, Y.; Ma, Z.; Su, W.; Wang, Q.; Wang, X.; Zhang, H. Analysis of Research Status of CO<sub>2</sub> Conversion Technology Based on Bibliometrics. *Catalysts* 2020, 10, 370.
  10. Panagiotopoulou, P. Methanation of CO<sub>2</sub> over alkali-promoted Ru/TiO<sub>2</sub> catalysts: II. Effect of alkali additives on the reaction pathway. *Appl. Catal. B Environ.* 2018, 236, 162–170.
  11. Rasheed, T.; Shafi, S.; Anwar, M.T.; Rizwan, K.; Ahmad, T.; Bilal, M. Revisiting Photo and Electrocatalytic Modalities for Sustainable Conversion of CO<sub>2</sub>. *Appl. Catal. A Gen.* 2021, 623, 118248.
  12. Aldana, P.U.; Ocampo, F.; Kobl, K.; Louis, B.; Thibault-Starzyk, F.; Daturi, M.; Bazin, P.; Thomas, S.; Roger, A. Catalytic CO<sub>2</sub> valorization into CH<sub>4</sub> on Ni-based ceria-zirconia. Reaction mechanism by operando IR spectroscopy. *Catal. Today* 2013, 215, 201–207.
  13. Aziz, M.; Jalil, A.; Triwahyono, S.; Sidik, S. Methanation of carbon dioxide on metal-promoted mesostructured silica nanoparticles. *Appl. Catal. A Gen.* 2014, 486, 115–122.
  14. Budi, C.S.; Wu, H.-C.; Chen, C.-S.; Saikia, D.; Kao, H.-M. Ni Nanoparticles Supported on Cage-Type Mesoporous Silica for CO<sub>2</sub> Hydrogenation with High CH<sub>4</sub> Selectivity. *ChemSusChem* 2016, 9, 2326–2331.
  15. Chen, H.; Liu, P.; Liu, J.; Feng, X.; Zhou, S. Mechanochemical in-situ incorporation of Ni on MgO/MgH<sub>2</sub> surface for the selective O-/C-terminal catalytic hydrogenation of CO<sub>2</sub> to CH<sub>4</sub>. *J. Catal.* 2021, 394, 397–405.
  16. Baysal, Z.; Kureti, S. CO<sub>2</sub> methanation on Mg-promoted Fe catalysts. *Appl. Catal. B Environ.* 2019, 262, 118300.
  17. Dębek, R.; Azzolina-Jury, F.; Travert, A.; Maugé, F. A review on plasma-catalytic methanation of carbon dioxide—Looking for an efficient catalyst. *Renew. Sustain. Energy Rev.* 2019, 116, 109427.
  18. Renda, S.; Ricca, A.; Palma, V. Precursor salts influence in Ruthenium catalysts for CO<sub>2</sub> hydrogenation to methane. *Appl. Energy* 2020, 279, 115767.

19. Li, L.; Wang, Y.; Zhao, Q.; Hu, C. The Effect of Si on CO<sub>2</sub> Methanation over Ni-xSi/ZrO<sub>2</sub> Catalysts at Low Temperature. *Catalysts* 2021, 11, 67.
20. Martínez, J.; Hernández, E.; Alfaro, S.; Medina, R.L.; Aguilar, G.V.; Albiter, E.; Valenzuela, M.A. High Selectivity and Stability of Nickel Catalysts for CO<sub>2</sub> Methanation: Support Effects. *Catalysts* 2018, 9, 24.
21. Tu, J.; Wu, H.; Qian, Q.; Han, S.; Chu, M.; Jia, S.; Feng, R.; Zhai, J.; He, M.; Han, B. Low temperature methanation of CO<sub>2</sub> over an amorphous cobalt-based catalyst. *Chem. Sci.* 2021, 12, 3937–3943.
22. Mateo, D.; Albero, J.; García, H. Titanium-Perovskite-Supported RuO<sub>2</sub> Nanoparticles for Photocatalytic CO<sub>2</sub> Methanation. *Joule* 2019, 3, 1949–1962.
23. Falbo, L.; Martinelli, M.; Visconti, C.G.; Lietti, L.; Bassano, C.; Deiana, P. Kinetics of CO<sub>2</sub> methanation on a Ru-based catalyst at process conditions relevant for Power-to-Gas applications. *Appl. Catal. B Environ.* 2018, 225, 354–363.
24. Liu, Q.; Bian, B.; Fan, J.; Yang, J. Cobalt doped Ni based ordered mesoporous catalysts for CO<sub>2</sub> methanation with enhanced catalytic performance. *Int. J. Hydrogen Energy* 2018, 43, 4893–4901.
25. Karelovic, A.; Ruiz, P. Mechanistic study of low temperature CO<sub>2</sub> methanation over Rh/TiO<sub>2</sub> catalysts. *J. Catal.* 2013, 301, 141–153.
26. Xu, X.; Liu, L.; Tong, Y.; Fang, X.; Xu, J.; Jiang, D.-E.; Wang, X. Facile Cr<sup>3+</sup>-Doping Strategy Dramatically Promoting Ru/CeO<sub>2</sub> for Low-Temperature CO<sub>2</sub> Methanation: Unraveling the Roles of Surface Oxygen Vacancies and Hydroxyl Groups. *ACS Catal.* 2021, 11, 5762–5775.
27. Dreyer, J.; Li, P.; Zhang, L.; Beh, G.K.; Zhang, R.; Sit, P.; Teoh, W.Y. Influence of the oxide support reducibility on the CO<sub>2</sub> methanation over Ru-based catalysts. *Appl. Catal. B Environ.* 2017, 219, 715–726.
28. Iqbal, M.M.A.; Abu Bakar, W.A.W.; Toemen, S.; Razak, F.I.A.; Azelee, N.I.W. Optimization study by Box-Behnken design (BBD) and mechanistic insight of CO<sub>2</sub> methanation over Ru-Fe-Ce/γ-Al<sub>2</sub>O<sub>3</sub> catalyst by in-situ FTIR technique. *Arab. J. Chem.* 2020, 13, 4170–4179.
29. Kim, H.Y.; Lee, H.M.; Park, J.-N. Bifunctional Mechanism of CO<sub>2</sub> Methanation on Pd-MgO/SiO<sub>2</sub> Catalyst: Independent Roles of MgO and Pd on CO<sub>2</sub> Methanation. *J. Phys. Chem. C* 2010, 114, 7128–7131.
30. Jiang, H.; Gao, Q.; Wang, S.; Chen, Y.; Zhang, M. The synergistic effect of Pd NPs and UiO-66 for enhanced activity of carbon dioxide methanation. *J. CO<sub>2</sub> Util.* 2019, 31, 167–172.
31. Ashok, J.; Pati, S.; Hongmanorom, P.; Tianxi, Z.; Junmei, C.; Kawi, S. A review of recent catalyst advances in CO<sub>2</sub> methanation processes. *Catal. Today* 2020, 356, 471–489.

32. Quindimil, A.; Bacariza, M.C.; González-Marcos, J.A.; Henriques, C.; González-Velasco, J.R. Enhancing the CO<sub>2</sub> methanation activity of  $\gamma$ -Al<sub>2</sub>O<sub>3</sub> supported mono- and bi-metallic catalysts prepared by glycerol assisted impregnation. *Appl. Catal. B Environ.* 2021, 296, 120322.
33. Yan, X.; Sun, W.; Fan, L.; Duchesne, P.N.; Wang, W.; Kübel, C.; Wang, D.; Kumar, S.G.H.; Li, Y.F.; Tavasoli, A.; et al. catalytic nanosheets for high-performance CO<sub>2</sub> methanation. *Nat. Commun.* 2019, 10, 2608–2618.
34. Pan, Q.; Peng, J.; Wang, S.; Wang, S. In situ FTIR spectroscopic study of the CO<sub>2</sub> methanation mechanism on Ni/Ce<sub>0.5</sub>Zr<sub>0.5</sub>O<sub>2</sub>. *Catal. Sci. Technol.* 2014, 4, 502–509.
35. Xu, X.; Tong, Y.; Huang, J.; Zhu, J.; Fang, X.; Xu, J.; Wang, X. Insights into CO<sub>2</sub> methanation mechanism on cubic ZrO<sub>2</sub> supported Ni catalyst via a combination of experiments and DFT calculations. *Fuel* 2020, 283, 118867.
36. Miao, B.; Ma, S.S.K.; Wang, X.; Su, H.; Chan, S.H. Catalysis mechanisms of CO<sub>2</sub> and CO methanation. *Catal. Sci. Technol.* 2016, 6, 4048–4058.
37. Huang, J.; Li, X.; Wang, X.; Fang, X.; Wang, H.; Xu, X. New insights into CO<sub>2</sub> methanation mechanisms on Ni/MgO catalysts by DFT calculations: Elucidating Ni and MgO roles and support effects. *J. CO<sub>2</sub> Util.* 2019, 33, 55–63.
38. Le, T.A.; Kim, J.; Kang, J.K.; Park, E.D. CO and CO<sub>2</sub> methanation over M (M Mn, Ce, Zr, Mg, K, Zn, or V)-promoted Ni/2O<sub>3</sub> catalysts. *Catal. Today* 2019, 348, 80–88.
39. Hasan, M.; Asakoshi, T.; Muroyama, H.; Matsui, T.; Eguchi, K. CO<sub>2</sub> methanation mechanism over Ni/Y<sub>2</sub>O<sub>3</sub>: An in situ diffuse reflectance infrared Fourier transform spectroscopic study. *Phys. Chem. Chem. Phys.* 2021, 23, 5551–5558.
40. Solis-Garcia, A.; Hernandez, J.F.; Almendarez-Camarillo, A.; Fierro-Gonzalez, J. Participation of surface bicarbonate, formate and methoxy species in the carbon dioxide methanation catalyzed by ZrO<sub>2</sub>-supported Ni. *Appl. Catal. B Environ.* 2017, 218, 611–620.
41. Westermann, A.; Azambre, B.; Bacariza, M.C.; Graça, I.; Ribeiro, M.F.; Lopes, J.M.; Henriques, C. Insight into CO<sub>2</sub> methanation mechanism over Ni/USY zeolites: An operando IR study. *Appl. Catal. B Environ.* 2015, 174–175, 120–125.
42. Lin, X.; Wang, S.; Tu, W.; Hu, Z.; Ding, Z.; Hou, Y.; Xu, R.; Dai, W. MOF-derived hierarchical hollow spheres composed of carbon-confined Ni nanoparticles for efficient CO<sub>2</sub> methanation. *Catal. Sci. Technol.* 2019, 9, 731–738.
43. Pan, Q.; Peng, J.; Sun, T.; Wang, S.; Wang, S. Insight into the reaction route of CO<sub>2</sub> methanation: Promotion effect of medium basic sites. *Catal. Commun.* 2013, 45, 74–78.
44. Younas, M.; Kong, L.L.; Bashir, M.J.K.; Nadeem, H.; Shehzad, A.; Sethupathi, S. Recent Advancements, Fundamental Challenges, and Opportunities in Catalytic Methanation of CO<sub>2</sub>.

Energy Fuels 2016, 30, 8815–8831.

45. Su, X.; Xu, J.; Liang, B.; Duan, H.; Hou, B.; Huang, Y. Catalytic carbon dioxide hydrogenation to methane: A review of recent studies. *J. Energy Chem.* 2016, 25, 553–565.
46. Jacquemin, M.; Beuls, A.; Ruiz, P. Catalytic production of methane from CO<sub>2</sub> and H<sub>2</sub> at low temperature: Insight on the reaction mechanism. *Catal. Today* 2010, 157, 462–466.
47. Italiano, C.; Llorca, J.; Pino, L.; Ferraro, M.; Antonucci, V.; Vita, A. CO and CO<sub>2</sub> methanation over Ni catalysts supported on CeO<sub>2</sub>, Al<sub>2</sub>O<sub>3</sub> and Y<sub>2</sub>O<sub>3</sub> oxides. *Appl. Catal. B Environ.* 2019, 264, 118494.
48. Zhou, G.; Liu, H.; Cui, K.; Jia, A.; Hu, G.; Jiao, Z.; Liu, Y.; Zhang, X. Role of surface Ni and Ce species of Ni/CeO<sub>2</sub> catalyst in CO<sub>2</sub> methanation. *Appl. Surf. Sci.* 2016, 383, 248–252.
49. Bukhari, S.N.; Chong, C.C.; Setiabudi, H.D.; Cheng, Y.W.; Teh, L.P.; Jalil, A.A. Ni/Fibrous type SBA-15: Highly active and coke resistant catalyst for CO<sub>2</sub> methanation. *Chem. Eng. Sci.* 2020, 229, 116141.
50. Cerdá-Moreno, C.; Chica, A.; Keller, S.; Rautenberg, C.; Bentrup, U. Ni-sepiolite and Ni-todorokite as efficient CO<sub>2</sub> methanation catalysts: Mechanistic insight by operando DRIFTS. *Appl. Catal. B Environ.* 2019, 264, 118546.
51. Liang, C.; Hu, X.; Wei, T.; Jia, P.; Zhang, Z.; Dong, D.; Zhang, S.; Liu, Q.; Hu, G. Methanation of CO<sub>2</sub> over Ni/Al<sub>2</sub>O<sub>3</sub> modified with alkaline earth metals: Impacts of oxygen vacancies on catalytic activity. *Int. J. Hydrogen Energy* 2019, 44, 8197–8213.
52. Zhou, R.; Rui, N.; Fan, Z.; Liu, C.-J. Effect of the structure of Ni/TiO<sub>2</sub> catalyst on CO<sub>2</sub> methanation. *Int. J. Hydrogen Energy* 2016, 41, 22017–22025.
53. Jia, X.; Zhang, X.; Rui, N.; Hu, X.; Liu, C.-J. Structural effect of Ni/ZrO<sub>2</sub> catalyst on CO<sub>2</sub> methanation with enhanced activity. *Appl. Catal. B Environ.* 2018, 244, 159–169.

Retrieved from <https://encyclopedia.pub/entry/history/show/48490>